Available online at www.sciencedirect.com
SCIENCE DIRECT®
Thin Solid Films 426 (2003) 238–245
thin solid films
www.elsevier.com/locate/tsf

In situ measurements of sensor film dynamics by spectroscopic ellipsometry. Demonstration of back-side measurements and the etching of indium tin oxide

I. Zudans, C.J. Seliskar*, W.R. Heineman

Department of Chemistry, University of Cincinnati, P.O. Box 210172, Cincinnati, OH 45221-0172, USA

Received 30 August 2002; received in revised form 7 January 2003; accepted 8 January 2003

Abstract

A new liquid flow cell design for in situ ellipsometric measurements on transparent multilayer samples using variable angle spectroscopic ellipsometry is presented. In this cell, films made on transparent substrates are in direct contact with liquid solution. Ellipsometry measurements are made through the transparent substrate, that is, from the back-side relative to the incident light so that films are in continuous contact with the liquid. This cell is not limited to just one angle of incidence of light allowing the films to be characterized at several angles before, during and after liquid contact. The spectral range of measurements is limited only by absorption of light in the underlying transparent substrate and not by the liquid solution that the film is in contact with. As a demonstration, we have measured and analyzed the dynamics of an indium tin oxide film on glass undergoing acid etching. Data from this in situ experiment were successfully modeled and the ITO layer thickness decreased uniformly during the etching process with an average etch rate of 0.23 nm/min.

Keywords: Ellipsometry; In situ; Indium tin oxide; Acid etching

1. Introduction

A focus of our research has been to design and develop new chemical sensors [1]. Typically, these sensors have consisted of an optical multilayer structure in which both optical and electrochemical events are monitored. In particular, spectroelectrochemical sensors have been developed [1,2] in which a transparent conducting indium tin oxide (ITO) coated glass substrate has been over-layered with thin films of a variety of different chemically selective porous optical materials. Sensing was achieved by attenuated total reflection spectroscopy of electrochemically modulated oxidation–reduction couples at the ITO-selective film interface. We have typically used [3] chemically selective films that have been prepared using sol–gel processed silica composites. In this process, ion exchange polymers were added to the sol–gel precursor solution before spin coating to obtain the necessary optical and chemical properties of the resulting film.

The chemically selective film is an essential part of the sensor. Yet, relatively little is currently known about the detailed behavior of these films in solution while sensing occurs at the ITO–film interface. Under harsh chemical conditions, for example in strongly alkaline solutions, the spectroelectrochemical sensor fails in time apparently due to the dissolution and/or delamination of the chemically-selective film. In other cases, these films undergo significant volume and refractive index changes as analyte partitions into and out of them. In seeking ways to understand sensor performance, including sensor failure, we have begun to explore ellipsometry.

Single wavelength ellipsometry has been successfully used to study interfacial processes at electrode surfaces [4,5]. Variable angle spectroscopic ellipsometry [6,7] has the potential to determine the changes in optical constants (refractive index and extinction coefficient) and thickness of multilayer film structures in our sensors. Hilfiker et al. demonstrated the use of spectroscopic

*Corresponding author. Tel.: +1-513-556-9200; fax: +1-513-556-9239.
E-mail address: Carl.Seliskar@uc.edu (C.J. Seliskar).

0040-6090/03/$ - see front matter © 2003 Elsevier Science B.V. All rights reserved.
PII: S0040-6090(03)00029-4

ellipsometry to monitor electrodeposition of Ni on Cu [8] and deposition of Ni and Cu layers on gold [9]. They were able to model the growth of these layers and determine optical constants of deposited layers from in situ experiments. Arwin [10] has reviewed use of spectroscopic ellipsometry in biological systems, including monitoring processes at solid–liquid interfaces. In this review Arwin describes a commonly used liquid cell and its limitations for in situ ellipsometric studies. Discussion of various liquid cell designs has also been given by Hilfiker [11]. Such a cell typically consists of a liquid reservoir with windows for incident and reflected light. The solid sample is immersed in this reservoir creating the liquid–solid interface that is interrogated optically. Entrance and exit windows need to be perpendicular to the light beams to avoid window-induced polarization changes. This configuration thus limits measurements to one pre-designed angle of incidence. In this cell configuration, light passes through solution resulting in measurements that can be made only in parts of the spectrum where solution does not absorb [8]. In application to sensors systems, this last characteristic meant that we would not be able to monitor changes in optical constants of chemically selective films in the wavelength regions of most interest to us, namely, in the region of analyte optical absorption.

In an effort to measure chemically-selective thin film properties in time, and indirectly sensor response, we have begun to explore using dynamic spectroscopic ellipsometry. In this paper, we present the details of a method to measure the dynamics of sensor films illustrating it with an application to the etching of indium tin oxide. This process is important in the patterning of indium tin oxide films for electronic devices including sensors. We felt that before studying more complex systems it was important to demonstrate that data for a model system with known transformations could be interpreted correctly. An ITO film was chosen as the model system in part because the film composition does not change during the course of the experiment; only its thickness changes. These ITO films are uniform across the sample and, therefore, it was also possible to test for such effects as stress induced in the sample by the cell. The solution that was used to etch ITO was yellow (contained iron) and would clearly absorb light on the short end of the experimental spectrum, thus, further demonstrating the usefulness of back-side measurements.

2. Experimental

2.1. Chemicals and materials

Chemicals used are 5.0 M HCl (Labchem), $FeCl_3 \cdot 6H_2O$ (Fisher Scientific), methanol (HPLC grade, Fisher Scientific). Deionized water was prepared with Barnstead water purification system and was used to prepare all solutions. Acid solution used for etching was 0.01 M $FeCl_3$ in 0.5 M HCl. ITO-coated Corning 1737 F glass sheets (20 $\Omega/\square$) were purchased from Thin Film Devices and cut into 1- by 3-inch pieces (also referred to as slides). Gaskets were cut from silicone sheeting (0.010-inch thick, gloss/gloss surface, Specialty Manufacturing). Nalgene 50 silicone tubing (0.125 inch ID $\times$ 0.250 inch OD, Fisher Scientific) was used to deliver solutions into the liquid cell. The liquid cell was made of black Delrin and was surface polished with 400 grit and 600 grit papers (Buehler).

2.2. Cleaning of the slides

Prior to use, slides were lightly wiped with lens paper soaked with methanol, rinsed with deionized water and cleaned with Isoclean® cleaning solution (Isolab). As a final step, slides were flushed with deionized water and dried by pulling lens paper over the surfaces.

2.3. Instrumentation

A J.A. Woollam Inc. variable angle spectroscopic ellipsometer (vertical setup) was used for all ellipsometric measurements. This instrument was equipped with an adjustable retarder (Auto Retarder®) that permitted measurement of Ψ and Δ in their full range (0–90° and 0–360°, respectively), and also enabled measurements of the depolarization of the light. Depolarization data were included in all analysis. J.A. Woollam Inc. Wvase32 software was used for modeling ellipsometric data. Collected data were modeled using published techniques [6,7]. Goodness of fit was expressed as mean squared error (M.S.E.) between experimental and predicted data (normalized by the S.D.s of experimental data). Thus, a smaller M.S.E. value represents better agreement between experimental and predicted data. A Philips XL30 ESEM was used to acquire surface images of native and etched ITO coated slides.

3. Results and discussion

3.1. Ellipsometry cell design

Because of the constraints imposed by previous cell designs, a new design was developed that allowed measurements of the sensor selective film in contact with solutions. The overall positioning of the cell within the ellipsometer is shown in Fig. 1. The cell sits in the normal position with respect to the source (P) and detector (D). The sample configuration itself differs from previous designs in that the film of interest (L2) is interrogated from the 'back-side' or substrate (L1) side as detailed in Fig. 1, inset. This configuration

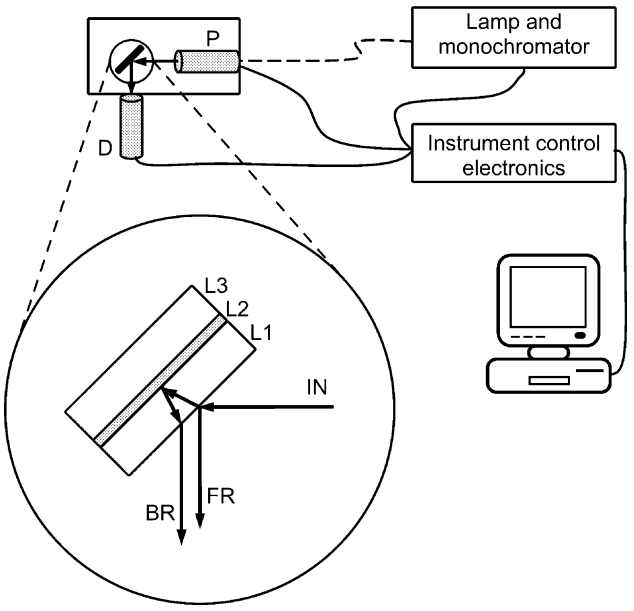

Fig. 1. Schematic of the variable angle spectroscopic ellipsometer set-up used in this study with an expanded view of sample slide containing multilayer structure. Insert shows light path in the sample and principle of the back-side measurement. Solid lines illustrate electrical control cables. Light from monochromator is guided to the polarizer (P) via optical cable (dotted line). Light reflected off the sample passes through analyzer and is detected by detector (D). In the expanded view, a three-layer optical system is illustrated. For back-side configuration the first layer incident light (IN) will strike the first layer (L1). Some of the light is reflected at this first interface (FR) and the rest goes into the substrate. The studied film (L2) and solution (L3) is on the back-side of substrate. Some of the light that was transmitted into the substrate will be reflected at the back surfaces (glass/film and film/solution interfaces) of the substrate and will come out of the slide (BR), the rest is transmitted into the solution. Reflection from the front surface does not contain information about the film but the back reflection does. If glass substrate is thin (as in Section 2 of this paper), both beams are not fully spatially separated and both enter the detector.

permits an additional liquid phase (L3) to be in contact with the film. Importantly, a special liquid flow cell has been made to bring the film in contact with solution. The optics are also sketched in Fig. 1 inset. Light reflected from the front surface (FR) does not contain information about the interior layers. Some light is transmitted into the substrate and reflected at layers within the sample including the back surface in contact with the liquid phase (L3). This fraction of the reflected beam (BR) contains information about film and liquid solution. Johs et al. [12] present a mathematical description of such an optical system where reflections from back-side of a transparent substrate have to be included in the analysis. They also give an example of how measurements from back-side can be used to complement studies of complex absorbing films. As described by Johs et al. [12] reflections from the front of the substrate are treated as incoherent with respect to the reflections from the back of the substrate.

There are several advantages of this configuration compared with more conventional cell designs. Interrogating light does not pass through a thick solution layer and, therefore, the solution (unlike in conventional cells) can absorb light at the wavelength of measurement. Measurements can be made at all wavelengths where the substrate (in this case, glass and ITO) itself does not absorb significantly. The angle of incidence of the interrogating light is not limited to one pre-designed angle. For the same sample, measurements can be made at several different angles of incidence without reconfiguring the sample and cell holder. Even though the angle of light with respect to sample normal at the glass/film surface is different from that at the air/glass interface, it still varies appreciably and this is also manifested in collected data. For example, at 60° incidence (for a wavelength of 550 nm) on the outside surface, the variation of the angle by 1° produces a variation of approximately 0.4° at the inner surface. Experimentally, a variation of 2° at the glass/film interface is easily attained. Such an angle variation causes significant changes in collected data. In addition, there are no windows through which light passes permitting data to be analyzed directly without correction for window effects. However, care must be taken to ensure that optical birefringence is not induced from stress residing in sample surfaces.

The details of the liquid flow cell are presented in Fig. 2. The cell consists of two main pieces with cell assembly as shown. The back piece has a parallelogram shaped cavity with two access ports where silicone tubes are inserted for liquid flow. The front piece serves as a support for the sample that is placed over and completely covers the opening to the liquid cavity in the back piece. This front piece has an aperture cut out of its center to permit measurements. Soft silicone gaskets are placed between the sample (typically a flat transparent piece 1×3 inches) and both cell parts to ensure a hermetic seal to the back piece while minimizing stress-induced birefringence that results from tightening of the screws (eight matching holes) that hold the whole assembly in place. To minimize stress-induced birefringence, both cell pieces were fine polished to ensure that all surfaces that contact the sample were flat.

As others have noted [11], stress induced in the sample by the cell is of special concern. After the cell was made, we tested it with ITO-coated glass slides. Our strategy was to collect data from a well-defined sample in a conventional way before placing it in the liquid cell. Comparison of this baseline data with data from the same sample in the liquid cell without liquid was then made. Ideally, both sample configurations should lead to the same results within experimental error. Initially, we struggled with this and after consid-

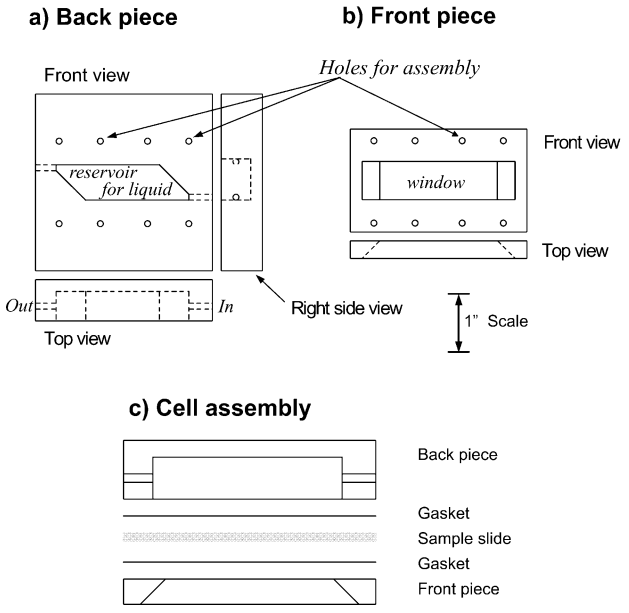

Fig. 2. Liquid cell drawings for back-side ellipsometric measurements. (a) Back piece—view from front, above and right. There is a parallelogram shaped cavity in the center of this piece where sample is exposed to solution when cell is assembled. Silicone tubing (not shown) is inserted in injection ports labeled In and Out. (b) Front attachment piece—view from front and above. The cut out center window of this piece allows measurements from its side in assemble cell. Front and back pieces have eight matching holes for screws that hold these pieces together. All dimensions are to scale. (c) Scheme of cell assembly.

erable testing, we concluded that even though immediately after machining and polishing all cell surfaces were flat, plastic materials like Delrin deform over time after machining giving surfaces that become slightly curved. In turn, these warped surfaces induce stress in the sample when it is put in the cell. Such small cell surface deformations were able to be essentially eliminated by continued surface polishing during the first months after cell machining. Ultimately, cell surface deformation stopped.

Once the cell was essentially stress-free, data were collected for the ITO slide mounted in the cell (no liquid) and ex situ, that is, without the cell holder. Comparison of the two data sets showed that differences were small but slightly larger than 1 S.D. of the measurements. Maximum deviations of 0.15° Ψ and 7° Δ were observed; however, the overall difference in Δ was less than 1.5°. Ex situ experiments were repeated several times after slightly changing the spot where light strikes the sample. Differences among data collected at these various points were similar to those observed when comparing ex situ experiment and sample in-the-cell data sets. Because of this, we have concluded that main cause for these differences lies in ITO layer variations per se and not stress-induced in the sample by the liquid cell. Another copy of the liquid cell was made from aluminum where samples might be studied in solutions that do not react with this metal. As expected, the aluminum liquid cell appeared to be less prone to inducing stress in the sample. Once the source of stress in the sample was identified and eliminated, we had no major problems with the liquid cell design. Alignment of the liquid cell is more straightforward than with a conventional cell since there are no windows that light passes through leading to necessary corrections of experimental data [13].

As noted in Fig. 1, the front surface reflection (FR) in our experiments does not contain information about the film on the back-side of the sample. Yet, this reflection is of higher intensity than reflections coming from interior layers including the back-side of the substrate where the film is. Therefore, a logical improvement in use of this design would be to block this front reflection from entering the detector. The diameter of the light beam for our instrument is approximately 4 mm. If the glass substrate thickness was increased to at least that amount, the back reflection could be spatially separated from front surface reflection and by itself directed into the detector. Our simulations also indicate that such measurements would be more sensitive to changes in film's properties on the back-side of the sample. Calculations show that for p-polarized light for film-free back surface (end of the etching), the FR reflection is at least two times more intense than the intensity of beams reflected from the back surfaces. For s-polarized light, the intensity differences are even more dramatic, e.g. the front reflection is at least 20 times more intense. ITO film's presence on the back surface improves light reflection from the back surface and for p-polarized light, depending on film's thickness and the wavelength, the front reflection can be even smaller than the intensity of light coming from the back surfaces. During the ITO etching process these conditions gradually change from one case to the other. Overall, in the case of ITO etching, adequate sensitivity was observed since ITO optical constants are very different from the glass substrate and the acid solution's constants. However, in future use with sensor films, this is an issue since these films are often optically very similar to glass or the solution phase and such sensitivity improvements would be welcome.

3.2. Demonstration of concept

To demonstrate that it was indeed possible to measure a film's changes with the cell configuration we chose an experiment where the optical changes were known before the experiment. The chosen system was ITO film acid etching. ITO films on glass substrates have been extensively studied by spectroscopic ellipsometry [14] and references therein [15,16]. Acid etching of these

Table 1
Refractive index values for materials

Wavelength nm	1737 F glass	1737 F glass*	ITO *n*	ITO *k*	Water** *n*
375	1.5359		2.1283	0.0024	1.3540
400	1.5330		2.0782	0.0022	1.3500
425	1.5304		2.0409	0.0026	1.3470
450	1.5280	1.5267	2.0100	0.0032	1.3440
475	1.5259		1.9829	0.0038	1.3420
500	1.5240	1.5228	1.9585	0.0045	1.3390
525	1.5222		1.9356	0.0053	1.3380
550	1.5206	1.5203	1.9139	0.0061	1.3360
575	1.5192		1.8929	0.0071	1.3340
600	1.5178	1.5180	1.8723	0.0081	1.3330
625	1.5166		1.8519	0.0093	1.3320
650	1.5155	1.5164	1.8314	0.0105	1.3310
675	1.5144		1.8108	0.0119	1.3300
700	1.5135	1.5150	1.7899	0.0134	1.3290
725	1.5126		1.7686	0.0151	1.3280
750	1.5118	1.5137	1.7469	0.0169	1.3270

* From Corning data for 1737 F glass.
** From Palik [21].

films is widely used for production of flat screen displays. Different aspects of this process have been studied [17–20]. In practice, etching solutions typically completely dissolve ITO films within a few minutes. Halogen acids are most effective for such fast etching. A literature survey indicated that HCl solutions that contain a small amount of Fe^{3+} yield the most uniform etching and a smooth ITO surface. The rate of the etching can be adjusted by changing the acid concentration. Considering all these factors, we decided to use a low concentration HCl solution containing Fe^{3+} that should result in a slow uniform etching of ITO. Under these conditions, only the ITO film thickness would be a variable in the measurement. In other words, etching would be observed as changes in ellipsometric parameters that later could be used to determine the film's thickness in time.

3.2.1. Optical constants of materials

Optical constants of all layers were first studied ex situ and are summarized in Table 1. The following procedure for ellipsometry was used. Corning 1737 F base glass was measured and its optical constants were determined. ITO coated slides were studied using the liquid cell before and after water was injected in the cell; both data sets were fitted together to arrive at the best set of ITO constants and film thickness. When these data were fitted, the base glass layer parameters were kept fixed at previously determined values. The refractive index of water was taken from the literature [21]. Water's refractive index was compared to that of acid solution using an Abby refractometer. Comparison indicated that the real part of the refractive index of the acid solution was higher by 0.0045 units. Such small differences would be hard to detect with the current optical system and, therefore, in all cases, the refractive index of pure water was used for the acid etching solution.

Experimental conditions and optical models used to fit experimental data are summarized in Table 2 where the layers in optical models, the wavelength range, the angle of incidence and the M.S.E. of the model for representative data sets are given. Optical constants for surface layers (SR) were calculated using the Bruggeman Effective Medium Approximation where the layer (glass or ITO) on which this surface layer was placed was mixed with the adjacent layer (air or water). When a particular layer's optical constants were fitted, the entry in Table 2 for this layer is italicizied. Layer thickness is shown in bold when it was allowed to vary during fitting. When the cell layers described in Table 2 span several data sets, (e.g. 0.7-mm glass layer), these layers were identical in fitting these separate sets. Water layers were included in models as infinitely thick layers. Scans 2 and 3 were fitted together and, therefore, one M.S.E. is given. M.S.E. is not given for the dynamic experiment because each time slice of data was fitted separately for ITO thickness and had its own M.S.E. (from 2 to 10, average value <5).

The refractive index of the base glass (1737 F) was determined from an uncoated glass sample. Spectroscopic scans from 300 to 1100 nm with step size 10 nm were performed at angles from 56 to 57° by 0.2°. The optical model included the following layers: surface roughness (0.3 nm)–1737 F glass (1 mm)–surface

Table 2
Instrument scan and model parameters for ex situ and dynamic ellipsometry

	Surface roughness nm	1737 F glass mm	ITO thickness nm	Surface roughness nm	Water layer	Scan range (interval) nm	Scan angles (interval)	M.S.E.
Scan 1	0.3	*1.1*	No	**0.3**	No	300–1100 (10)	56 to 57 (0.2)	0.4
Scan 2	0.4		***130.0***	**3.3**	No		54 to 62 (2)	2.7
Scan 3		0.7			Yes			
Dynamic scans	0.4		**Var**	No	Yes	375–750 (25)	60	–

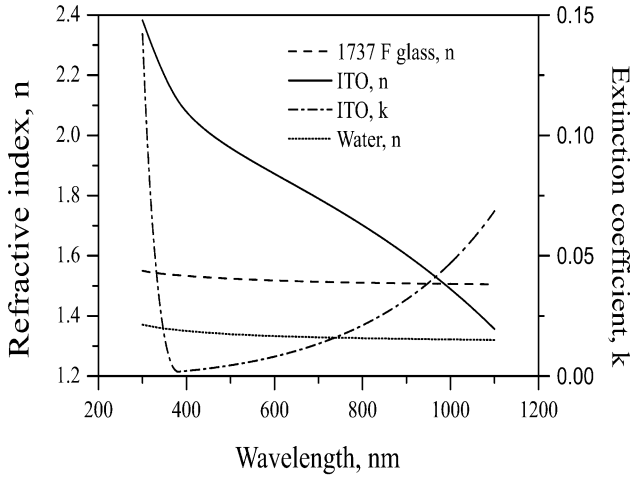

Fig. 3. Optical constants (n and k) of various optical layers. Glass and ITO constants were determined from experiments prior dynamic etching studies. Refractive index of water was taken from the literature [21].

roughness (0.3 nm). Data were fit with a M.S.E. of 0.4. Optical constants for water were taken from Palik [21] except that a small constant value of k (10^{-8}) was assumed for the entire spectral range for software functioning reasons.

Prior to etching, each ITO slide was characterized as follows. Spectroscopic scans were made from 300 to 1100 nm with a step size of 10 nm at angles from 54 to 62° with an interval size of 2°. After that water was injected into the cell and data collected under identical conditions. The ITO layer was assumed to have uniform optical constants through its thickness and an oscillator model was used to model its optical constants. Including a small surface roughness layer on ITO significantly improved the quality of the fit. We feel that its inclusion is justified since such a surface roughness layer can be observed in SEM images of the surface. Such images have also been reported in the literature [18]. An oscillator model was used for ITO that included a Drude oscillator for near-IR absorbtion, a Tauc–Lorentz oscillator at 5.3 eV and a pole for ε_1 offset. The latter was used to account for the influence of absorption at short wavelengths on the refractive index in the visible region of the spectrum.

The optical model was as follows: glass surface roughness (0.4 nm)–1737F glass (0.7 mm)–ITO (130 nm)–ITO surface roughness (3.3 nm). Both data sets (dry cell and with water) were fit simultaneously. This model yielded a small M.S.E. (2.7 for particular data set presented) and small correlation coefficients between fit parameters and self-consistent optical constants. Optical constants of all layers are presented in Fig. 3 and in Table 1 for wavelengths used in dynamic ellipsometry experiments. Table 1 also lists refractive index values for 1737F glass from the manufacturers data sheets and these are in good agreement with our experimentally determined values. It is well known that ITO optical constants vary with manufacturer, deposition process and annealing conditions. Our determined values overall are similar in wavelength distribution and magnitude to previously published values [14–16].

3.2.2. Dynamics of acid etching of ITO

Brewster's angle for the base glass–water interface is to within a few tenths of a degree of 57° in the spectral range used (300–1100 nm). For glass samples, when ellipsometric measurements are made very close to Brewster's angle, the data are highly sensitive to any surface imperfections. As a result, a surface roughness layer of 0.3 nm was included on each glass surface because inclusion of them significantly improved the match between calculated and experimental data (lowers M.S.E.). A few degrees above this angle such effects are negligible and the measurements are still very sensitive to thickness of the relatively high refractive index ITO (compared to glass) film. Thus, for etching studies an angle of incidence of 60° was chosen. This angle is slightly above Brewster's angle and, therefore, after ITO is removed the measured Δ will be zero for all wavelengths. To speed up data collection, the acquisition range for dynamic measurements was narrowed to 375–750 nm with a 25-nm interval. A scan at these 16 wavelengths was performed with an average time of 2.2 min. The acid concentration for etching was tuned so that within this scan time the ITO thickness did not change significantly (as discussed later this was 0.23 nm/min change) and so complete ITO removal was achieved within a reasonable time (1 day). Our current instrumentation permitted dynamic data to be acquired only at one angle of incidence at a time. However, prior to a dynamic experiment the same sample spot was characterized at multiple angles. Such a capability will be very important when sensor film dynamics will be studied. The demonstrated measurement configuration allows detailed sample characterization at multiple angles prior to dynamic experiments and after film processes have reached equilibrium without changing the spot monitored on the sample. Conventional liquid cells do not allow such a possibility. All data analyses were done after the experiment was completed.

Each individual scan of 16 wavelengths was later analyzed as if all points were measured at the time the first point was measured (time slice). Thickness of the ITO layer at this time was determined by fitting this portion of complete data set. Optical model for analysis of dynamic data included three layers—glass surface roughness layer, 1737 F glass substrate layer, ITO film layer and an acid solution (infinite) layer. ITO surface roughness was not included in the model—this omission made the fit of the data only slightly worse but simpli-

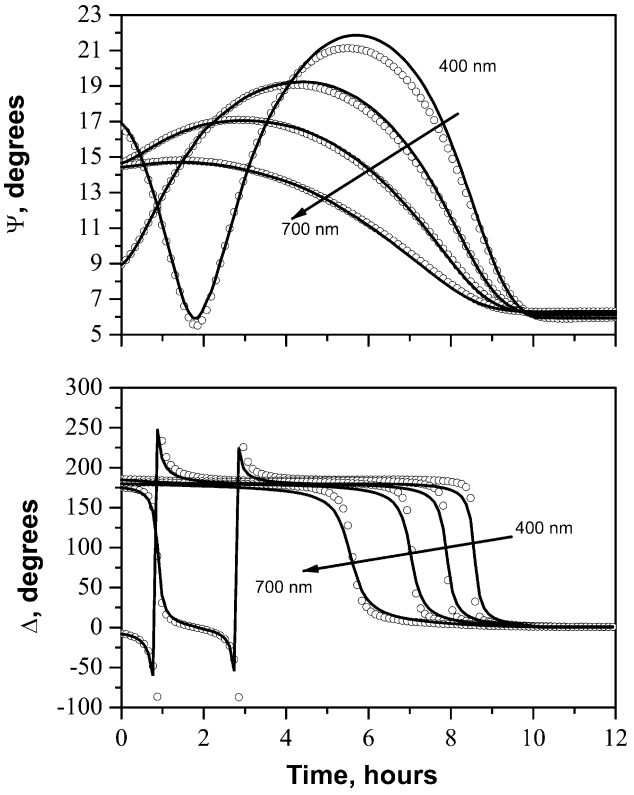

Fig. 4. Measured (circles) and calculated (solid lines) data from model with fitted thickness. For simplicity, data at only four wavelengths (in nm: 400, 500, 600 and 700) are presented which cover different parts of the spectrum. For fitting, the complete data set was used. Experimental and calculated values at other wavelengths matched comparably well to data presented. Depolarization was also measured and included in fitting process but data are not presented. It also matched calculated data. Arrows point to data series in increasing wavelength direction. In the Δ graph, the discontinuity from low delta values to high is artificial. Δ Is a continuous 360° function and only for graphing purposes it is discontinued at −90° and continues at 270° (these two points are the one and same point in polar coordinates).

fied the fitting procedure for dynamic data. Optical constants of all layers were determined as described before and were kept constant for this part of experiment. The only parameter in this optical model that was allowed to vary was thickness of the ITO layer. After the ITO slide with water was characterized, water was drained from the cell and the acid etching solution was injected. Dynamic data acquisition was started immediately after injection. Fig. 4 presents experimental data that were collected over time at selected wavelengths along with model fitted results. It can be seen that the experimental data and the model generally agree well. The fitted ITO thickness as a function of etching time is presented in Fig. 5. It shows that ITO thickness decreased uniformly with time. The middle portion of this curve (from 1 to 8 h) was fitted with linear regression which yielded an etch rate of 0.23 nm/min and $R^2 = 0.9998$.

It is evident from examining Fig. 4 that calculated data do not agree exactly with experimental data. Even though the overall shapes of curves agree well in most regions, some deviations are relatively large. Specifically, computed values of Ψ differ significantly from experiment at short wavelengths; computed Δ values from experiment at 6–9 h in time. We attribute this disagreement to use of an oversimplified ITO layer model. Our experiment was not designed to describe the etching process as accurately as possible. Instead, it was meant to demonstrate the concept of measuring film dynamics on the back-side of glass. We omitted a surface roughness layer from the model for fitting dynamic data. Our ex situ modeling indicates that it is certainly present on ITO in the beginning of the experiment. We also used a simple model for ITO with uniform optical constants throughout its thickness. Literature indicates that these films often have vertical composition gradients through its thickness that result in graded optical constants [15]. Our ex situ experiments generally are consistent with such observations. Such differences are especially evident at near-IR wavelengths [15]. In the visible part of the spectrum, these effects are small and for modeling simplicity of dynamic data, ITO can be approximated as a uniform layer.

4. Conclusions

In this paper we have presented a liquid flow cell design for use with a variable angle spectroscopic ellipsometer. In this cell, films made on transparent substrates are in direct contact with solution. Ellipsometry measurements are made through the substrate—the film and solution are on the back-side of the substrate relative to incident light. This cell is not limited to just

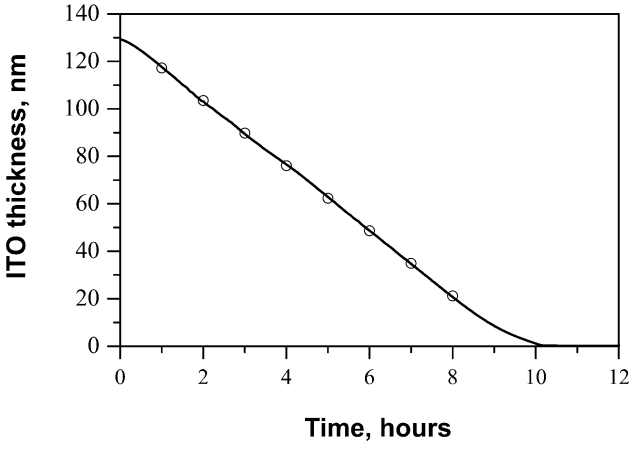

Fig. 5. Fitted ITO layer thickness during the course of the dynamic experiment. Solid line represents determined thickness at each time slice of the data set. Circles mark the linear fit region.

one angle of incidence of light allowing the sample film to be characterized at several angles before, during and after a dynamic experiment. The spectral range of experiments is limited only by absorbtion of the light in the underlying glass and not by the solution that the film is in contact with. We have demonstrated that film dynamics in solution can be studied in such a configuration by measuring the acid etching of an ITO film on glass. Data from this in situ experiment were successfully modeled and the ITO layer of a thickness change over time was determined. The ITO thickness uniformly decreased during the etching process and the average etch rate was determined to be 0.23 nm/min.

Studies of the dynamics of chemically selective films on sensors are underway. Two aspects of these films need to be understood. Film stability over long periods of time in solution is, in general, of concern for some film compositions. Another aspect is film dynamics in analyte solutions. For our multilayer optical sensor, it is important to understand how the film's optical constants and thickness are changing as a sensor functions. As has been demonstrated here with ITO acid etching, the described liquid flow cell is well suited for this task.

Acknowledgments

This work was supported by a grant awarded by the Environmental Management Sciences Program of the US Department of Energy, Office of Environmental Management (Grant DE-FG0796ER62331). The purchase of the J.A. Woollam Inc. ellipsometer and Philips ESEM was made possible by a grant from the Hayes Fund of the State of Ohio. The authors thank Sean Conklin for ESEM measurements. Comments on the manuscript by J.A. Woollam and J.N. Hilfiker were greatly appreciated.

References

[1] Y. Shi, A.F. Slaterback, C.J. Seliskar, W.R. Heineman, Anal. Chem. 69 (1997) 3679.
[2] Y. Shi, C.J. Seliskar, W.R. Heineman, Anal. Chem. 69 (1997) 4819.
[3] Y. Shi, C.J. Seliskar, Chem. Mater. 9 (1997) 821.
[4] S. Gottesfeld, in: A.J. Bard (Ed.), Electroanalytical Chemistry, 15, Marcel Dekkar, New York, 1989, p. 143.
[5] S. Gottesfeld, Yeon-Tak Kim, A. Redendo, in: I. Rubinstein (Ed.), Physical Electrochemistry: Principles, Methods and Applications, Marcel Dekkar, New York, 1995, p. 393.
[6] J.A. Woollam, B. Johs, C.M. Herzinger, J. Hilfiker, R. Synowicki, C.L. Bungay, Crit. Rev. Opt. Sci. Technol. CR72 (1999) 3.
[7] J. Blaine, J.A. Woollam, C.M. Herzinger, J. Hilfiker, R. Synowicki, C.L. Bungay, Crit. Rev. Opt. Sci. Technol. CR72 (1999) 28.
[8] J.N. Hilfiker, D.W. Thompson, J.S. Hale, J.A. Woollam, Thin Solid Films 270 (1995) 73.
[9] J.N. Hilfiker, D.W. Glenn, S. Heckens, J.A. Woolam, J. Appl. Phys. 79 (1996) 6193.
[10] H. Arwin, Thin Solid Films 313–314 (1998) 764.
[11] J.N. Hilfiker, M.S. Theses, Electrical Engineering, University of Nebraska, USA, Nebraska, USA, 1995.
[12] B. Johs, R.H. French, F.D. Kalk, W.A. McGahan, J.A. Woollam, Proc. SPIE 2253 (1994) 1098.
[13] B. Johs, J. Hale, N.J. Ianno, C.M. Herzinger, T. Tiwald, J.A. Woollam, Proc. SPIE 4449 (2001) 41.
[14] J.A. Dobrowolski, L. Li, J.N. Hilfiker, Appl. Opt. 38 (1999) 4891.
[15] R.A. Synowicki, Thin Solid Films 313–314 (1998) 394.
[16] T. Gerfin, M. Grätzel, J. Appl. Phys. 79 (1996) 1722.
[17] M. Scholten, J.E.A.M. van den Meerakker, J. Electrochem. Soc. 140 (1993) 471.
[18] J.E.A.M. van den Meerakker, P.C. Baarslag, M. Scholten, J. Electrochem. Soc. 142 (1995) 2321.
[19] T.J. Vink, W. Walrave, J.L.C. Daams, P.C. Baarslag, J.E.A.M. van den Meerakker, Thin Solid Films 266 (1995) 145.
[20] J.E.A.M. van den Meerakker, P.C. Baarslag, W. Walrave, T.J. Vink, J.L.C. Daams, Thin Solid Films 266 (1995) 152.
[21] Edward D. Palik (Ed.), Handbook of Optical Constants of Solids II, Academic Press, Boston, 1991.